Mesoscale Analysis of Size Effect on Mechanical Properties of Concrete

Muttaqin Hasan
Dept. Of Civil Engineering, Syiah Kuala University, Banda Aceh, Indonesia
Email: muttaqin@unsyiah.ac.id

Sri Indah Setiyaningsih
Dept. of Civil Engineering, Muhammadiyah Aceh University, Banda Aceh, Indonesia
Email: sriindahsetiyaningsih@yahoo.co.id

***Abstract*—This paper presents mesoscale analysis on mechanical properties of concrete that has different size by two dimensional Rigid Body Spring Model (RBSM). The specimens used in this analysis are cylinders with diameter /height (mm): 50/50, 50/100, 50/150, 50/200, 100/100, 100/200, 100/300, 100/400, 150/150, 150/300, 150/450, and 150/600. Nominal maximum sizes of aggregate were 9.5 mm, 25 mm, and 30 mm with grain size distribution according to JSCE Standard. The aggregate distributed randomly into the analyzed models. The loading conducted with deformation control with the increment of 0.005 mm for compression analysis and 0.0005 mm for tension analysis. Compressive strength, tensile strength and elastic modulus of all specimens with the same of *h*/*d*, decrease with the increasing of nominal maximum size of aggregate. For all specimens with the same nominal maximum size of aggregate, compressive strength, tensile strength and elastic modulus decrease with increasing of concrete slenderness (*h*/*d*).**

***Index Terms*—size effect, mesoscale, rigid body spring method, maximum aggregate size, specimen slenderness, mechanical properties of concrete**

I. Introduction

In recent years, research at the meso level from the analytical point of view has begun, but has not been conducted far enough yet. The analysis of compression test in particular has hardly been carried out due to complicated failure behavior involved [1]-[4]. At the meso level, in which concrete is considered as composite material with three phases: aggregate, mortar and interface, Nagai *et al.*, was successly simulated failure mechanism and failure modes of mortar and concrete specimens using both two and three dimensional method [5], [6].

The study on size effect on mechanical properties was conducted mainly by experimental approach [7]-[12]. In this paper, the mesoscale analysis using two dimensional Rigid Body Spring Model (RBSM) on the size effect on mechanical properties of concrete is presented. The analysis was conducted in both tension and compression. The study parameters were the maximum size of aggregate and the slenderness ratio of the concrete specimens. Twelve series of concrete cyclinder specimens with different maximum aggregate size and different specimens dimension were analyzed.

The objective of this study is to obtain the effect of maximum aggregate size and slenderness ratio of concrete specimens on tensile strength, compressive strength and modulus of elasticity of concrete. The formula to predict concrete strength in tension and compression at different slenderness ratio is proposed as a function of the specimen slenderness ratio based on the data obtained in the analysis.

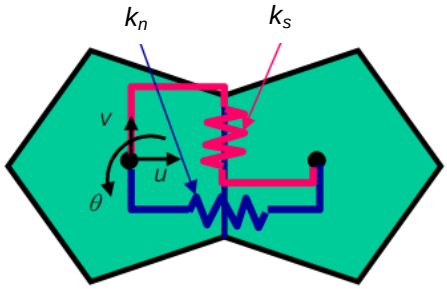

Figure 1. Elements, spring and degress of freedom

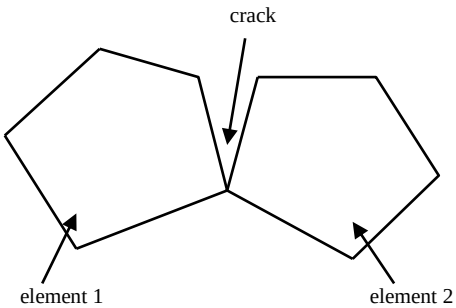

Figure 2. Crack in elements

II. Rigid Body Spring Model

Rigid Body Spring Model (RBSM) is a discrete numerical analysis method first developed by Kawai [13], [14]. The analytical model is devided into polyhedron

Manuscript received April 20, 2015; revised August 5, 2015.

doi: 10.18178/ijscer.4.3.265-270

elements whose boundaries are interconnected by two springs, called normal and shear spring as shown in Fig. 1. Each element has two translational and one rotational degrees of freedom at the center of gravity. Cracks initiate and propagate along the boundary (Fig. 2). A mesh arrangement of random geometry using Voronoi diagram is used. [15]. A geometric computational program developed by Sugihara is applied [16].

Normal and shear elastic moduli are calculated by assuming a plane stress condition as follows [5].

$$k_n = \frac{E}{1-\nu^2} \quad (1)$$

$$k_s = \frac{E}{1+\nu} \quad (2)$$

where k_n and k_s = elastis modulus of normal and shear spring; E and ν = elastic modulus and Poisson's ratio of element. Material constants (E, ν) at the aggregate-mortar interface are calculated as in Fig. 3 [17].

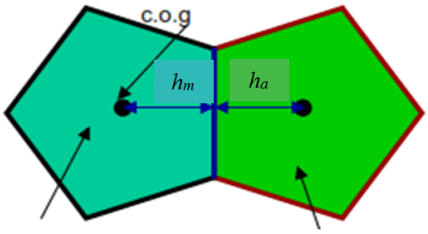

$$E = (E_m h_m + E_a h_a)/(h_m + h_a)$$

$$\nu = (\nu_m h_m + \nu_a h_a)/(h_m + h_a)$$

Figure 3. Material constant at interface

III. Mesoscale Constitutive Model

The mesoscale constitutive models developed by Nagai *et al.* [5] and Ueda *et al.* [17] were used in this study. Nagai et. al. assumed that no fracturing occurs in compression dan the tensile strength of the mortar and it interfaces has a normal distribution with the following probability density function [5].

$$f(f_t) = \frac{1}{s\sqrt{2\pi}} \exp\left\{-\frac{(f_t-\bar{\mu})^2}{2s^2}\right\} \quad (3)$$

$$s = -0.2\bar{\mu} + 1.5$$

where f_t = element tensile strength, when $f_t < 0$ then, $ft = 0$; μ = average value of element tensile strength; and s = standard deviation. The same distribution was assumed for normal and shear spring.

The elasto-plastic and fracture behavior was adopted for normal spring. When the normal spring of mortar or interface elements reaches its tensile strength, the elements get fracture, then the normal stress decreses linierly with increasing crack width. The maximum crack width at which the tensile stress can be transferred has a distribution depending on the tensile strength and corresponding crack width. In compression, the spring always behave elastically. The unloading and reloading path does not pass through the origin, but has some plasticity. The plasticity increases and the stiffness decreases as the strain at the unloading point increases. A linear unloading-reloading path that follows the envelope stress-strain curve in compression at a strain of ε_{pa} is adopted as shown in Fig. 4 [17].

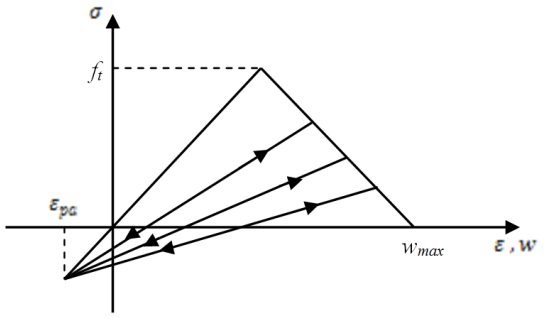

Figure 4. Unloading-reloading path

The elasto-plastic model was adopted for shear spring [5]. Shear stress is proportional to shear strain until it reaches a maximum value (τ_{max}) and then remains constant at τ_{max} as shear strain increases further. The τ_{max} criteria developed by Ueda et. al. [17] and Tailor and Brom and Kosaka *et al.* [18], [19] were used for mortar and interface respectively as follows:

For mortar:

$$\tau_{max} = \pm(f_t + 0{,}11f_t^3(-\sigma + f_t)^{0{,}6}) \quad (4)$$

For interface:

$$\tau_{max} = \pm(-\sigma\tan\emptyset + c) \quad (5)$$

The aggregate elements are assumed to behave elastically without fracturing [5].

IV. Analitical Method

A. Analitical Model

Twelve series of analitical model were used. The analized models were concrete cylinder specimens with different maximum aggregate size, which are 12,5 mm, 25 mm and 30 mm. The diameter of cylinder specimens for maximum aggregate size of 12,5 mm, 25 mm and 30 mm were 50 mm, 100 mm and 150 mm, respectively. The specimen with 50 mm dimeter has the height of 50 mm, 100 mm, 150 mm and 200 mm. The specimen with 100 mm dimeter has the height of 100 mm, 200 mm, 300 mm and 400 mm. The specimen with 150 mm dimeter has the height of 150 mm, 300 mm, 450 mm and 600 mm.

The aggregate was distributed randomly in the model. The grain size distribution of aggregate was based on JSCE Standard [20]. The circular aggregate was used in the analytical model. The aggregate distributed into the model in the following ways (see Fig. 5):

- Set the maximum size of aggregate first into the model, followed by the smaller one, etc.
- Centroid of the aggregate is located in the model randomly. Aggregate can be drawn by inserting its radius.

- To locate the next aggregate centroid, check that the distance between that centroid and the already stored centroids should satisfy the condition in the Fig. 5.

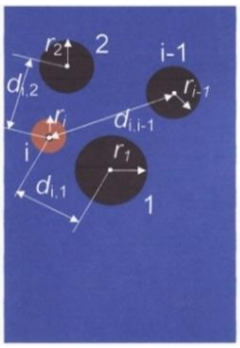

$$d_{i,1} - (r_i + r_1) \geq k$$
$$d_{i,2} - (r_i + r_2) \geq k$$
$$d_{i,i-1} - (r_i + r_{i-1}) \geq k$$
$$k = positive\ constant$$

Figure 5. Set up aggregate into the model

B. Element Meshing

Element meshing was conducted by Voronoi diagram. Voronoi points were distributed randomly in the analyzed model. Distribution of Voronoi points is conducted in such a way to have almost uniform size of polygon. Width and height of analyzed model were divided into some square elements. Each element contains one Voronoi point and poligons were able to construct. In this study the number of elements was limited to 2400.

C. Analytical Process

The program developed by Nagai *et al*. was used in the analysis [5]. The stiffness matrix was constructed based on the principal of virtual work [14]. The modified Newton-Raphson method was used as the convergence algorithm. In the convergence process, displacement canceling the unbalanced forces of elements was added to the elements. The displacements were calculated using the stiffness matrix. Convergence of the model was judged when the ratio of the summed squares of unbalanced forces to the summed squares of applied forces fall below 10^{-5}. Displacement of loading boundary was controlled. The deformation increment of 0.005 mm and 0,0005 mm was set for compression and tension analysis, respectively. The input material properties as shown in Table I was used.

TABLE I. INPUT MATERIAL PROPERTIES

Parameters	Mortar	Aggregate	Interface
f_c' (MPa)	4,0	NA[1)]	1,8
E (GPa)	25,0	50,0	-
ν	0,18	0,25	-
c (MPa)	-	-	3,0
ϕ (°)	-	-	35

[1)] It is assumed that the aggregate does not facture

V. ANALITICAL RESULTS

A. Compression Analysis Results

The mechanical properties for all specimens under compression are summarized in Table II. The values in Table II are the average value of 3 specimens conducted in the analysis for each series.

TABLE II. MECHANICAL PROPERTIES OF CONCRETE UNDER COMPRESSION

Series	Maximum Aggregate Size (mm)	Cylinder Size, d/h (mm)	Compressive Strength (MPa)	Modulus of Elasticity (GPa)
1	9,5	50/50	45.8	22.6
2	9,5	50/100	40.9	22.0
3	9,5	50/150	36.0	20.0
4	9,5	50/200	30.2	16.5
5	25	100/100	41.6	20.5
6	25	100/200	37.9	19.0
7	25	100/300	32.0	18.8
8	25	100/400	26.0	14.7
9	30	150/150	37.9	18.0
10	30	150/300	32.8	16.5
11	30	150/450	27.3	14.2
12	30	150/600	22.4	12.6

Fig. 6 and Fig. 7 show the relationship of compressive strength, modulus of elasticity and the maximum aggregate size. From those figures, it can be seen that the compressive strength and modulus of elasticity decrease with the increase in the maximum aggregate size. This is similar with experimental finding [11].

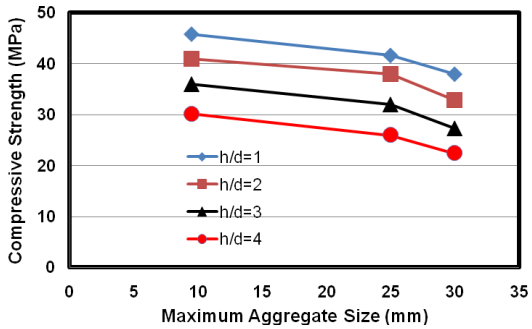

Figure 6. Relationship between compressive strength and maximum aggregate size

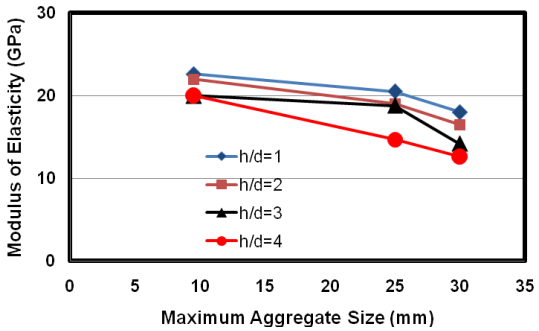

Figure 7. Relationship between modulus of elasticity in compression and maximum aggregate size

The relationship between compressive strength, modulus of elasticity and specimen slenderness (*h*/*d*) are shown in Fig. 8 and Fig. 9. From those figure, it can be seen that compressive strength and modulus of elasticity decrease with the increase in specimen slenderness. This is also similar with experimental finding [11]. The relationship between compressive strength and specimen slenderness is almost linear.

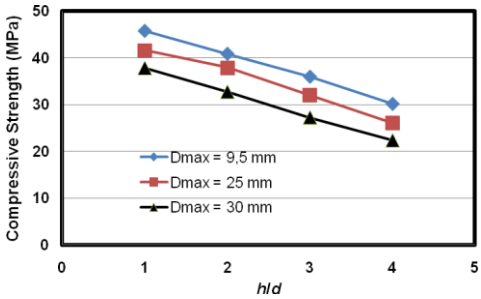

Figure 8. Relationship between compressive strength and specimen slenderness (*h*/*d*)

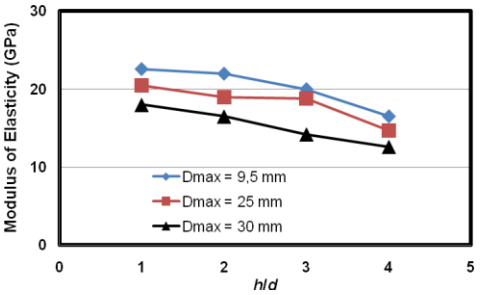

Figure 9. Relationship between modulus of elasticity in compression and specimen slenderness

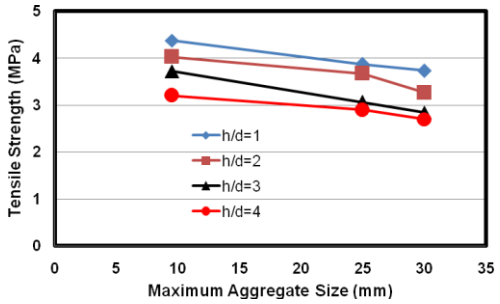

Figure 10. Relationship between tensile strength and maximum aggregate size

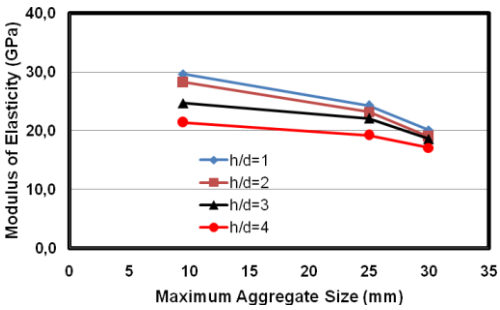

Figure 11. Relationship between modulus of elasticity in tension and maximum aggregate size

B. *Tension Analysis Results*

The mechanical properties for all specimens under tension are summarized in Table III. The values in Table III are the average value of 3 specimens conducted in the analysis for each series.

TABLE III. MECHANICAL PROPERTIES OF CONCRETE UNDER TENSION

Series	Maximum Aggregate Size (mm)	Cylinder Size, d/h (mm)	Tensile Strength (MPa)	Modulus of Elasticity (GPa)
1	9,5	50/50	4.4	29.6
2	9,5	50/100	4.0	28.2
3	9,5	50/150	3.7	24.7
4	9,5	50/200	3.2	21.4
5	25	100/100	3.9	24.3
6	25	100/200	3.7	23.2
7	25	100/300	3.1	22.1
8	25	100/400	2.9	19.3
9	30	150/150	3.7	20.1
10	30	150/300	3.3	19.0
11	30	150/450	2.8	18.6
12	30	150/600	2.7	17.1

Fig. 10 and Fig. 11 show the relationship of tensile strength, modulus of elasticity and the maximum aggregate size. From those figures, it can be seen that the tensile strength and modulus of elasticity decrease with the increase in the maximum aggregate size. This is similar with experimental finding [11].

The relationship between tensile strength, modulus of elasticity and specimen slenderness (*h*/*d*) are shown in Fig. 12 and Fig. 13. From those figure, it can be seen that tensile strength and modulus of elasticity decrease with the increase in specimen slenderness. This is also similar with experimental finding [11].

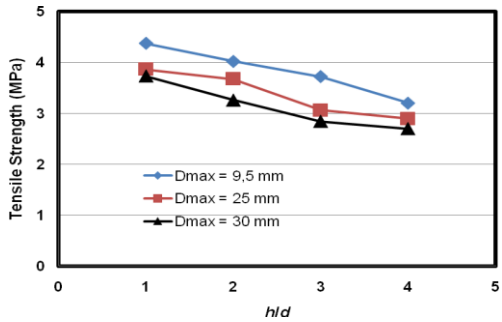

Figure 12. Relationship between tensile strength and specimen slenderness

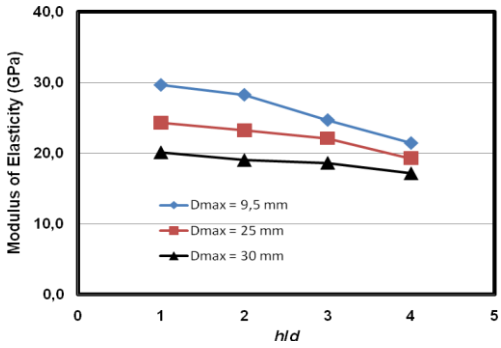

Figure 13. Relationship between modulus of elasticity in tension and specimen slenderness

C. *Specimen Size Effect on Concrete Strength*

To see the specimen size effect on concrete strength, the tensile strength and compressive strength of concrete obtained in this analysis are normalized with the tensile strength and compressive strength for specimen with slenderness ratio (*h*/*d*) of 2,0 for which usually use in the test for determining concrete strength. The result is

shown in Fig. 14. The same trendline for different specimen diameter both in tension and compression was found. By using linear regression analysis, the slenderness effect on the strength of concrete can be written as follows:

$$\frac{\sigma}{\sigma_{2,0}} = 1{,}24\left(\frac{h}{d}\right) - 0.12 \quad (6)$$

where σ = concrete strength at any specimen slenderness; $\sigma_{2,0}$ = concrete strength at h/d = 2,0; h = the height of specimen; and d = the diameter of specimen.

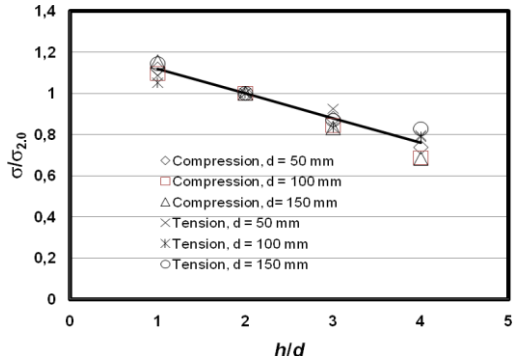

Figure 14. The specimen size effect on concrete strength

D. *Relationship between Modulus of Elasticity, Tensile Strength and Compressive Strength*

The relationship between modulus of elasticity and compressive strength, modulus of elasticity and tensile strength, tensile strength and compressive strength are shown in Fig. 15, Fig. 16, and Fig. 17 respectively.

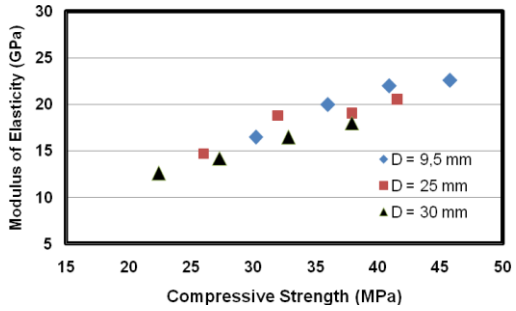

Figure 15. Relationship between modulus of elasticity and compressive strength

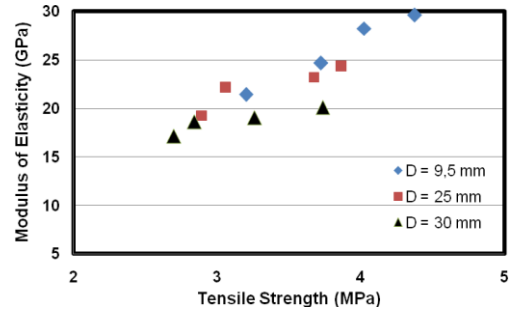

Figure 16. Relationship between modulus of elasticity and tensile strength

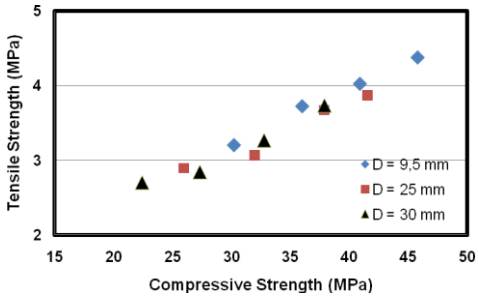

Figure 17. Relationship between tensile strength and compressive strength

VI. Conclusions

Mesoscale analysis on concrete cylinder specimens under tension and compression with different specimen size and different maximum aggregate size was carried out. The following conclusions are drawn from this research:

- Compressive strength, tensile strength and modulus of elasticity decrease with the increase in maximum aggregate size
- Compressive strength, tensile strength and modulus of elasticity decrease with the increase in slenderness of specimen
- The strength of concrete at any specimen slenderness was proposed to have a linear relationship with the specimen slenderness.

Acknowledgment

The authors acknowledge the financial support provided for this study by Syiah Kuala University Graduate School Program.

References

[1] K. Nagai, Y. Sato, and T. Ueda, "Numerical simulation of fracture process of plain concrete by rigid body spring method (RBSM)," *Proceeding of the First Fib Congress, Concrete Structure in 21st Century*, vol. 8, pp. 99-106, 2002.

[2] P. Stroeven and M. Stroeven, "Space approach to concrete's space concrete structure and its mechanical properties," *Heron*, vol. 46, no. 4, pp. 265-269, 2001.

[3] M. Asai, K. Terada, K. Ikeda, H. Suyama, and K. Fujii, "Mesoscopic numerical analysis of concrete structures by a modified lattice model," *J. Struct. Mech. Earthquake Eng.*, vol. 731, no. 1, pp. 19-30, 2003.

[4] Z. P. Bazant, F. C. Caner, L. Cedolin, G. Gusatis, and G. D. Luzio, "Fracturing material models based micromechanical concept," *Proceedings of FraMCoS*, pp. 83-89, 2004.

[5] K. Nagai, Y. Sato, and T. Ueda, "Mesoscopic simulation of failure of mortar and concrete by 2D RBSM," *J. Adv. Concr. Tech.*, vol. 2, no. 3, pp. 359-374, 2004.

[6] K. Nagai, Y. Sato, and T. Ueda, "Mesoscopic simulation of failure of mortar and concrete by 3D RBSM," *J. Adv. Concr. Tech.*, vol. 3, no. 3, pp. 385-402, 2005.

[7] Z. P. Bazant, M. T. Kazemi, T. Hasegawa, and J. Mazars, "Size effect on brazilian split-cylinder tests: Measurement and fracture analysis," *ACI. Mat. J.*, vol. 88, no. 3, pp. 325-332, 1991.

[8] Z. P. Bazant, "Size effect on structural strength," *Springer Materials*, pp. 225-725, 1999.

[9] B. L. Karihaloo and Q. Z. Xiao, "Size effect in the strength of concrete structure," *Sadhana*, vol. 27, no. 4, pp. 449-459, 2002.

[10] U. Trende and O. Buyukozturk, "Size effect of aggregate roughness in interface fracture of concrete composite," *ACI Mat. J.*, vol. 95, no. 4, pp. 331-338, 1998.
[11] A. A. Youssif, M. A, Issa, M. S. Islam, and S. A. Issa, "Specimen and aggregat size effect on concrete compresive strength," *J. Cem. Concr. and Aggr.*, vol. 22, no. 2, 2000.
[12] J. K. Kim and S. T. Yi, "Application of size effect to compressive strength of concrete members," *Sadhana*, vol. 27, no. 4., pp. 467-484, 2002.
[13] T. Kawai, "New element models in discrete structural analysis," *J. Society of Naval Architect of Japan*, vol. 141, pp. 187-193, 1977.
[14] T. Kawai and N. Takeuchi, "Discrete limit analysis program, series of limit analysis by computer 2," Baifukan, Tokyo, 1990.
[15] A. Okabe, B. Boots, K. Sugihara, and S. N. Chiu, *Spatial Tessellations – Concepts and Applications of Voronoi Diagrams*, 2nd ed, New York: Wiley, 2000.
[16] K. Sugihara, *Fortran Computional Geometry Programming*, Tokyo: Iwanami Shoten, 1998.
[17] T. Ueda, M. Hasan, K. Nagai, Y. Sato, and L. Wang, "Meso-scale simulation of influence of frost damage on mechanical properties of concrete," *J. Mat. Civil. Eng.*, pp. 244-252, 2009.
[18] M. A. Taylor and B. B. Broom, "Shear bond strength between coarse aggregate and cement paste and mortar," *ACI J.*, vol. 61, no. 8, pp. 939-952, 1964.
[19] Y. Kosaka, Y. Tanigawa, and M. Kawakami, "Effect of coarse aggregate on fracture of concrete (Part 1)," *AIJ J.*, vol. 2228, pp. 1-11, 1975.
[20] JSCE, Standard Speccification for Concrete Structures – 2002: Materials and Construction, 6.2.5.3 Grading, JSCE Guidelines for Concrete, Japan Society of Civil Engineers, 2005.

Muttaqin Hasan is a lecturer and researcher at Department of Civil Engineering, Syiah Kuala University, Banda Aceh, Indonesia. He received his Bachelor in Civil Engineering at Department of Civil Engineering, Syiah Kuala University in 1989. Then he received Master in Material and Structural Engineering at Bandung Istititute of Tecnology in 1998. Later, he reveived PhD degree in Structural and Geotechnical Engineering at Hokkaido University, Japan in 2003. During 2003 – 2005 he conducted research as JSPS Postdoctoral Fellow at Division of Built Environment, Hokkaido University. His research areas include fatigue and fracture of concrete, behavior of concrete structures under severe environment, meso-scale analysis of concrete, retrofitting of concrete structures, and performance of concrete and steel structures under earthquake load.

Sri Indah Setiyaningsih is a lecturer at Department of Civil Engineering, Muhammadiyah Aceh University, Banda Aceh, Indonesia. She received Master degree in Structural Engineering at Syiah Kuala University. Now, she is pursuing PhD degree at Bandung Institute of Technology. Her reasearch areas include analysis of concrete materials and structures in meso level and behavior of concrete under severe environment.